





RESEARCH PAPER

Hyperpolarized [1-¹³C]pyruvate combined with the hyperinsulinaemic euglycaemic and hypoglycaemic clamp technique in skeletal muscle in a large animal model

Mads Bisgaard Bengtsen¹  | Esben Søvsø Szocska Hansen² |
Rasmus Stilling Tougaard³  | Mads Dam Lyhne³  | Nikolaj Fibiger Rittig^{1,4} |
Julie Støy⁴ | Niels Jessen⁴ | Christian Østergaard Mariager² |
Hans Stødkilde-Jørgensen² | Niels Møller¹ | Christoffer Laustsen² 

¹ Department of Endocrinology and Internal Medicine, Aarhus University Hospital, Aarhus N, Denmark

² The MR Research Center, Aarhus University Hospital, Aarhus N, Denmark

³ Department of Cardiology, Aarhus University Hospital, Aarhus N, Denmark

⁴ Steno Diabetes Center Aarhus, Aarhus University Hospital, Aarhus N, Denmark

Correspondence

Mads Bisgaard Bengtsen, Aarhus University Hospital, Department of Endocrinology and Internal Medicine, Palle Juul-Jensens Boulevard 99, 8200 Aarhus N, Denmark.
Email: madsbengtsen@clin.au.dk

Funding information

Aarhus Universitets Forskningsfond; Innovation Fund Denmark, Grant/Award Number: 1308-00028B

Edited by: Philip Atherton

Abstract

In skeletal muscle, glucose metabolism is tightly regulated by the reciprocal relationship between insulin and adrenaline, with pyruvate being at the intersection of both pathways. Hyperpolarized magnetic resonance (hMR) is a new approach to gain insights into these pathways, and human trials involving hMR and skeletal muscle metabolism are imminent. We aimed to combine the hyperinsulinaemic clamp technique and hMR in a large animal model resembling human physiology. Fifteen anaesthetized pigs were randomized to saline (control group), hyperinsulinaemic euglycaemic clamp technique (HE group) or hyperinsulinaemic hypoglycaemic clamp technique (HH group). Skeletal muscle metabolism was evaluated by hyperpolarized [1-¹³C]pyruvate injection and hMR at baseline and after intervention. The glucose infusion rate per kilogram increased by a statistically significant amount in the HE and HH groups ($P < 0.001$). Hyperpolarized magnetic resonance showed no statistically significant changes in metabolite ratios: [1-¹³C]lactate to [1-¹³C]pyruvate in the HH group versus control group ($P = 0.19$); and ¹³C-bicarbonate to [1-¹³C]pyruvate ratio in the HE group versus the control group ($P = 0.12$). We found evidence of profound increments in glucose infusion rates representing skeletal muscle glucose uptake, but interestingly, no signs of significant changes in aerobic and anaerobic metabolism using hMR. These results imply that hyperpolarized [1-¹³C]pyruvate might not be optimally suited to detect effects of insulin in anaesthetized resting skeletal muscle, which is of significance for future studies.

KEYWORDS

glucose metabolism, homeostasis, insulin, skeletal muscle

This is an open access article under the terms of the [Creative Commons Attribution-NonCommercial-NoDerivs](https://creativecommons.org/licenses/by-nc-nd/4.0/) License, which permits use and distribution in any medium, provided the original work is properly cited, the use is non-commercial and no modifications or adaptations are made.

© 2021 The Authors. *Experimental Physiology* published by John Wiley & Sons Ltd on behalf of The Physiological Society

1 | INTRODUCTION

The hyperinsulinaemic euglycaemic clamp technique is considered the gold standard when measuring the actions of insulin *in vivo* (DeFronzo et al., 1979). During a hyperinsulinaemic clamp, ~90% of the infused glucose is taken up by skeletal muscle (Thiebaud et al., 1982). After uptake, glucose is either converted to glycogen for later use or directed toward the glycolytic pathway, with pyruvate and lactate as the end-products. Pyruvate is incorporated into the citric acid cycle in aerobic conditions and converted into lactate in anaerobic conditions (DeFronzo & Tripathy, 2009; Jensen et al., 2011; Juel & Halestrap, 1999). These pathways are highly regulated by insulin.

Hyperpolarized magnetic resonance (hMR) is a new approach to obtain insights into fundamental metabolic pathways. The technique enables *in vivo* detection of injected hyperpolarized [1-¹³C]pyruvate and its conversion to its downstream metabolites, with a signal enhancement of > 10,000 in comparison to conventional magnetic resonance spectroscopy (Ardenkjær-Larsen et al., 2003).

Human trials involving hMR and skeletal muscle are imminent (Park et al., 2020; Torchi et al., 2019), and we investigated the impact of glucose homeostasis on resting muscle metabolism in a large animal model closely resembling human physiology (Swanson et al., 2004). Insulin stimulates muscle glucose uptake and glycolysis in humans (Shulman et al., 1990; Thiebaud et al., 1982), and it has been reported that insulin increases conversion of [1-¹³C]pyruvate to both [1-¹³C]lactate and [1-¹³C]alanine in rodent skeletal muscle (Leftin et al., 2013). Studies in striated cardiac muscle have also shown increased conversion of [1-¹³C]pyruvate to [1-¹³C]lactate and [1-¹³C]alanine after insulin stimulation (Hansen et al., 2017; Lauritzen et al., 2013), indicating increased metabolism. In addition, we and others have shown that hypoglycaemia increases blood lactate concentrations in humans, which is thought to be attributable to adrenaline stimulation of skeletal muscle and is destined for incorporation in hepatic gluconeogenesis (Bengtson et al., 2020; Gjedsted et al., 2011).

The present study was designed to test whether insulin exposure in the hyperinsulinaemic euglycaemic group would lead to detectable increases in [1-¹³C]lactate, [1-¹³C]alanine and ¹³C-bicarbonate signals in skeletal muscle compared with the control group, and whether hypoglycaemia in the hyperinsulinaemic hypoglycaemic group would lead to augmented conversion of [1-¹³C]pyruvate to [1-¹³C]lactate, assumed to be targeted to the liver as a gluconeogenic substrate.

2 | METHODS

2.1 | Ethical approval

The animal study conformed to the institutional guidelines laid down by the local animal welfare committee and was approved by the Danish Animal Experiments Inspectorate (2014-15-2934-01013). The pigs were anaesthetized with propofol *i.v.* (12 mg initial dose; thereafter, ~0.4 mg/kg/h for maintenance) and fentanyl *i.v.* (~8 µg/kg/h). In order to minimize stress to the animals, the degree of sedation was evaluated clinically by a health-care professional via constant video surveillance

New Findings

- **What is the central question of this study?**

Is it possible to combine the hyperpolarized magnetic resonance technique and the hyperinsulinaemic clamp method in order to evaluate skeletal muscle metabolism in a large animal model?

- **What is the main finding and its importance?**

The logistical set-up is possible, and we found substantial increments in glucose infusion rates representing skeletal muscle glucose uptake but no differences in ratios of [1-¹³C]lactate to [1-¹³C]pyruvate, [1-¹³C]alanine to [1-¹³C]pyruvate, and ¹³C-bicarbonate to [1-¹³C]pyruvate, implying that the hyperpolarization technique might not be optimal for detecting effects of insulin in skeletal muscle of anaesthetized animals, which is of significance for future studies.

and by continuous monitoring of haemodynamic parameters. At the end of the study day, animals were killed with a lethal dose of pentobarbital.

2.2 | Animals, handling and instrumentation

Fifteen healthy, female, Danish, domestic pigs (crossbreed of Landrace/Yorkshire/Duroc) weighing ~28–32 kg were included in this study. The animals were fed with standard feed but fasted from the night before experimental protocol. Each study day commenced at exactly 08.00 h upon arrival of the pigs, in order to reduce interference from diurnal variations in hormone fluctuation. An *i.v.* catheter was placed in the ear. The pigs were anaesthetized with propofol and fentanyl *i.v.*, intubated and mechanically ventilated with a 60% O₂-air mix using a commercially available Avance respirator system with a built-in CO₂ and O₂ gas monitoring unit (GE Healthcare, Broendby, Denmark). Minimally invasive *i.v.* catheterization was performed, guided by ultrasound, in the femoral artery and vein for the administration of hyperpolarized [1-¹³C]pyruvate, arterial blood pressure measurement, arterial and venous blood sampling and infusions. The pigs received saline infusions throughout the study day, and arterial blood gases were analysed frequently to ensure adequate ventilation and sedation.

2.3 | Design

Figure 1 illustrates the study protocol. Before the study day, the 15 pigs were randomized to three different intervention groups (five in

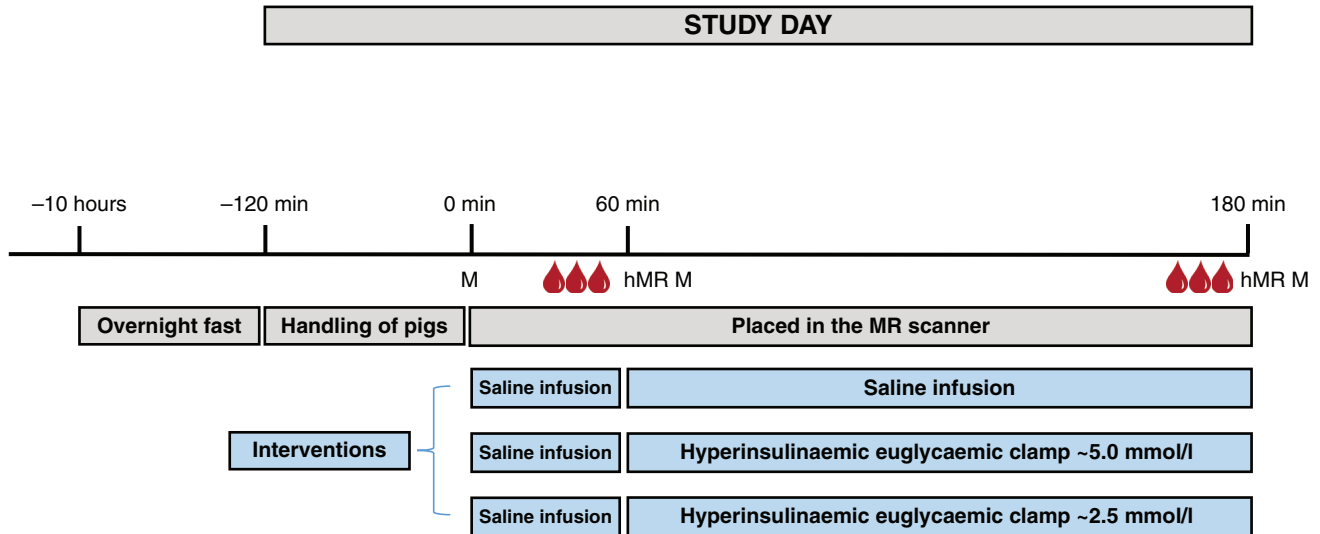


FIGURE 1 Schematic view of the study days. All pigs underwent an overnight fast and were allocated randomly to saline infusion (control group, $n = 5$), hyperinsulinaemic euglycaemic clamp (HE group, $n = 5$) or hyperinsulinaemic hypoglycaemic clamp (HH group, $n = 5$). Muscle biopsies are indicated by M, magnetic resonance hyperpolarization by hMR and triplicate blood sampling indicated by the red drops

each group) using Research Randomizer (www.randomizer.org). Each pig was allocated to saline infusion (control group), hyperinsulinaemic euglycaemic clamp (HE group) or hyperinsulinaemic hypoglycaemic clamp (HH group).

On the study day, after induction of general anaesthesia and instrumentation, the pigs were transported to the magnetic resonance (MR) scanner at ~10.00 h ($t = 0$ min). Long-line infusion lines were used because infusion pumps were not allowed in close proximity to the MR scanner. During the first hour (0–60 min) the pigs were acclimated to the MR scanner. At $t = 60$ min, one of the interventions commenced (saline infusion, hyperinsulinaemic euglycaemic glucose clamp or hyperinsulinaemic hypoglycaemic glucose clamp). The hyperinsulinaemic euglycaemic clamp was performed with a constant insulin infusion (1.0 mU/kg/min² Insulin Actrapid; Novo Nordisk, Copenhagen, Denmark) and a variable rate of 20% glucose infusion administered to maintain euglycaemia at ~5 mmol/l. Blood glucose was measured every 10 min. Likewise, the hyperinsulinaemic hypoglycaemic glucose clamp was performed with a constant insulin infusion (1.0 mU/kg/min) and a variable rate of 20% glucose infusion administered to maintain hypoglycaemia at ~2.5 mmol/l. Blood glucose was measured every 5–10 min. The glucose infusion rate per kilogram (a quantitative measure of i.v. glucose per body weight needed to maintain the desired glucose concentrations) was calculated. After the second scan, a gadolinium injection (Clariscan; GE Healthcare) was administered to assess blood flow to the muscle.

2.4 | Biochemical variables

Blood glucose was measured using a hand-held full blood glucose device (Contour XT; Bayer AG, Leverkusen, Germany), plasma lactate with the lactate oxidase method (YSI 2300 STAT plus; YSI Life

Sciences, Yellow Springs, OH, USA) and serum insulin with an enzyme-linked immunosorbent assay (Dako Denmark A/S, Glostrup, Denmark). Arterial blood samples were analysed with an ABL90 FLEX Plus (Radiometer Medical APS, Broenshoej, Denmark).

2.5 | Muscle biopsy and western blotting

Muscle biopsies from the biceps femoris were obtained with a 5 mm Bergström biopsy needle (Bergstrom, 1975). Biopsies were obtained from the left hindlimb at $t = 0$ min and at $t = 180$ min (after hMR). Biopsies were immediately frozen in liquid nitrogen. Stain-free protein technology (Gilda & Gomes, 2013) was used to demonstrate equal loading, and protein concentrations did not differ between groups. Image Lab 5.0 (Bio-Rad Laboratories) was used for visualization and quantification. The primary antibodies used were Akt (total, #4691 dilution 1:20000 and ser473, #9271 dilution 1:15000; Cell Signaling), GS (total, #3886 dilution 1:40000 and phosphorylated, #3891 dilution 1:30000; Cell Signaling) and As160 (total, #07-741 dilution 1:20000 and thr642 #4288 dilution 1:20000; Cell Signaling).

2.6 | Hyperpolarized probe preparation and dissolution

The hyperpolarized [$1\text{-}^{13}\text{C}$]pyruvate product was produced from the polarization of 641 mg of [$1\text{-}^{13}\text{C}$]pyruvic acid (density, 1.26 g/ml) mixed with 15 mM AH111501 (trisodium salt of tris{8-carboxyl-2,2,6,6-tetra[2-(1-methoxyethyl)]-benzo(1,2-d:4,5-d')bis(1,3)dithiole-4-yl}methyl acid; MW = 1595 g/mol) in a sterile polarizer (GE SpinLab; GE Healthcare) for 2.5 h at 5 T and 0.8 Kelvin, to ensure a reproducible polarization of > 40% on average. Dissolution was performed with 29 ml of de-ionized (18.2 mV) water in a receiver

syringe, containing 13 ml of 360 mM sodium hydroxide and 181 mM TRIS for neutralization of the pyruvic acid.

The time from dissolution to injection was on average 15 s. A bolus of 24 ml hyperpolarized [1-¹³C]pyruvate was given in the femoral vein and immediately flushed with 10 ml saline.

2.7 | ¹³C and ¹H MR scanning

The location of the left lower hindlimb and imaging position of the hyperpolarized pyruvate was ensured using a three-plane localizer centred on the position of the ¹³C coil and a ¹³C-lactate phantom positioned in the coil. The pigs were scanned twice with hyperpolarized [1-¹³C]pyruvate at predefined time points: $t = 60$ min (baseline) and $t = 180$ min (after interventions).

Magnetic resonance was performed on a clinical 3 T GE Discovery 750 MR scanner (GE Healthcare, Milwaukee, WI, USA). For the ¹³C spectroscopy and imaging, a set-up of a clamshell transmission coil and a surface loop receiver coil was used (both from Rapid Biomedical, Rimpfing, Germany). Bloch–Siegert experiments were performed before the ¹³C-pyruvate injection to estimate the central frequency and transmission power for the ¹³C spectrum and imaging. The ¹³C-spectral acquisition parameters were as follows: RF bandwidth = 2,000 Hz, spectral acquisition bandwidth = 5,000 Hz, number of samples = 2,048, TR = 1 s, time points = 128, flip angle = 12° and slice thickness = 40 mm (centred on the coil position in a perpendicular plane). One additional pig was included to acquire ¹³C images in the same set-up to verify the signal detection depth in the muscle. The dynamic images were acquired to obtain a 1 s resolution on [1-¹³C]pyruvate and 3 s on each individual metabolite {[1-¹³C]lactate, [1-¹³C]alanine and ¹³C-bicarbonate (H¹³CO₃⁻)}. Imaging acquisition was commenced at start of injection. The ¹³C-imaging acquisition parameters were two-dimensional spectral spatial excitation (80 Hz bandwidth) with spiral read-out in a saturation recovery approach, flip angle 8° for pyruvate and 90° for metabolites, in-plane resolution 8 mm × 8 mm, 40 mm slice over 2 min. Images were obtained with a repetition time of 500 ms between each acquisition.

2.8 | ¹³C and ¹H analysis

Hyperpolarized [1-¹³C]pyruvate spectral images were post-processed using software developed in house and an in-house adaptation of a published MATLAB script capable of localizing and integrating pyruvate and metabolites (Khegai et al., 2014). Conversion of [1-¹³C]pyruvate to metabolites was quantified as the ratios between summed integrals of [1-¹³C]pyruvate and metabolites. The first-pass muscle perfusion scans were analysed in the open-source software HOROS (v.2.4; The Horos Project) using the UMMPerfusion plugin (v.1.5.3) (Zöllner et al., 2016). Maps of muscle plasma flow were created using the model-free fast deconvolution approach, with a region of interest in the femoral artery defining the arterial input. The dynamic development from the signal in the ¹³C images was obtained in HOROS by delineating a region of interest covering the main signal from the muscle closest to the coil. The model uses a time-domain fit, using a

fixed model with a span of Lorentzian and Gaussian line shapes to fit the best line width and amplitude. This runs iteratively through the dataset for accurate peak assignment and fitting. Lastly, from the fitted spectra, a metabolic two-side exchange rate model is used in the frequency domain to fit the dynamics of pyruvate and its derivatives.

2.9 | Perfusion

Perfusion images [differential subsampling with cartesian ordering (DISCO)] was acquired in the same plane as the ¹³C spectral image, and the acquisition parameters were as follows: field of view = 340 mm × 340 mm, matrix = 160 × 128, PURE reconstruction, acceleration: phase = 2/slice = 1.5, number of samples = 2,048, echo time = 1.1/2.2, repetition time = 3.5 s, time points = 49, flip angle = 12°, number of slices = 24 and slice thickness = 4 mm.

2.10 | Statistics

Results are presented as the mean ± SD, unless otherwise specified. Graphs contain the mean with SD for normally distributed data and the median with 95% confidence intervals for non-normally distributed data. Normal distribution of data was ensured by the inspection of QQ plots, and data were logarithmically transformed if the distribution was unequal. Comparisons of consecutive measures were performed using two-way repeated-measures ANOVA and, when appropriate, with *post hoc* multiple comparison using the Holm–Sidak method when comparing the groups with one another. STATA v.13.0 (StataCorp, College Station, TX, USA) and SIGMAPLOT v.11 (San Jose, CA, USA) were used to perform statistical analyses and graphs. A *P*-value < 0.05 was considered statistically significant. The sample size was based upon our previous study examining cardiac muscle (Hansen et al., 2017).

2.11 | Outcomes

Outcomes for this study were metabolite ratios ([1-¹³C]lactate to [1-¹³C]pyruvate, [1-¹³C]alanine to [1-¹³C]pyruvate and ¹³C-bicarbonate to [1-¹³C]pyruvate ratios) measured with hMR spectroscopy. Additional outcomes were metabolite ratios (downstream metabolite by the sum of the downstream metabolites [1-¹³C]lactate, ¹³C-bicarbonate and [1-¹³C]alanine) to evaluate the metabolic fractional change (Nielsen et al., 2020), in addition to blood glucose, glucose infusion rates (GIR), serum insulin, plasma lactate and changes in insulin signalling in muscle biopsies in response to insulin stimulation.

3 | RESULTS

3.1 | Baseline characteristics

Fifteen pigs completed the study. *Post hoc* handling of data revealed that one pig in the control group had invalid MR spectroscopy data. Consequently, that pig does not contribute to MR spectroscopy data,

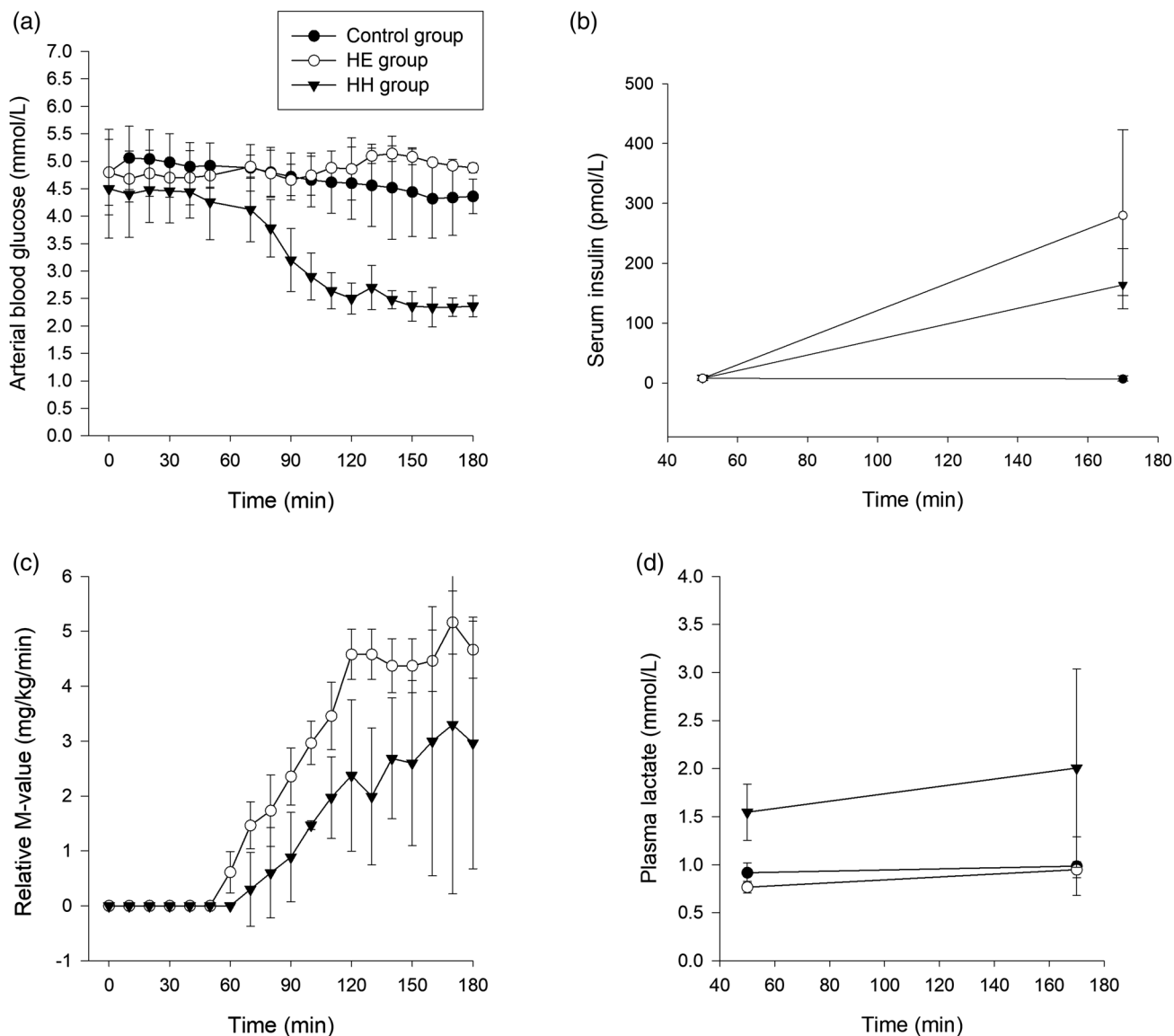


FIGURE 2 Glucose metabolism. A: Mean plasma glucose concentrations in mmol/L. B: Median serum-insulin concentrations in pmol/L with 95% CI. C: Glucose infusion rate presented as relative M-value (mg/kg/min). D: Mean plasma lactate concentrations in mmol/L

but contributes to the remaining data in the control group. This did not change the overall results. The three groups were comparable on weight (32.1 ± 3.4 kg in the control group, 29.6 ± 2.0 kg in the HE group and 30.3 ± 1.8 kg in the HH group; $P = 0.30$), baseline blood glucose (5.2 ± 0.8 , 5.1 ± 0.9 and 5.1 ± 0.4 mmol/l, respectively; $P = 0.97$) and baseline haemoglobin (6.1 ± 0.4 , 5.9 ± 0.8 and 6.2 ± 0.2 mmol/l, respectively; $P = 0.80$).

3.2 | Blood glucose concentrations

The blood glucose concentrations are illustrated in Figure 2a. The HE group had significant higher blood glucose compared with the control group from $t = 130$ min (interaction time \times group, $P = 0.03$). The HH group differed from the two other groups from $t = 60$ min

after commencement of the hyperinsulinaemic hypoglycaemic clamp (interaction time \times group, $P < 0.001$). During hypoglycaemia, blood glucose concentrations reached a nadir of $\sim 2.1 \pm 0.2$ mmol/l, and the duration of hypoglycaemia was 100 min (defined by blood glucose < 4.0 mmol/l).

3.3 | Insulin concentrations

No statistically significant differences were present in baseline insulin concentrations between the three groups ($P > 0.05$), as illustrated in Figure 2b. After commencement of clamps in the HE and HH groups, insulin concentrations increased to > 10 -fold in both groups compared with the control group (interaction group \times time, $P < 0.001$). No statistically significant difference in insulin concentration occurred

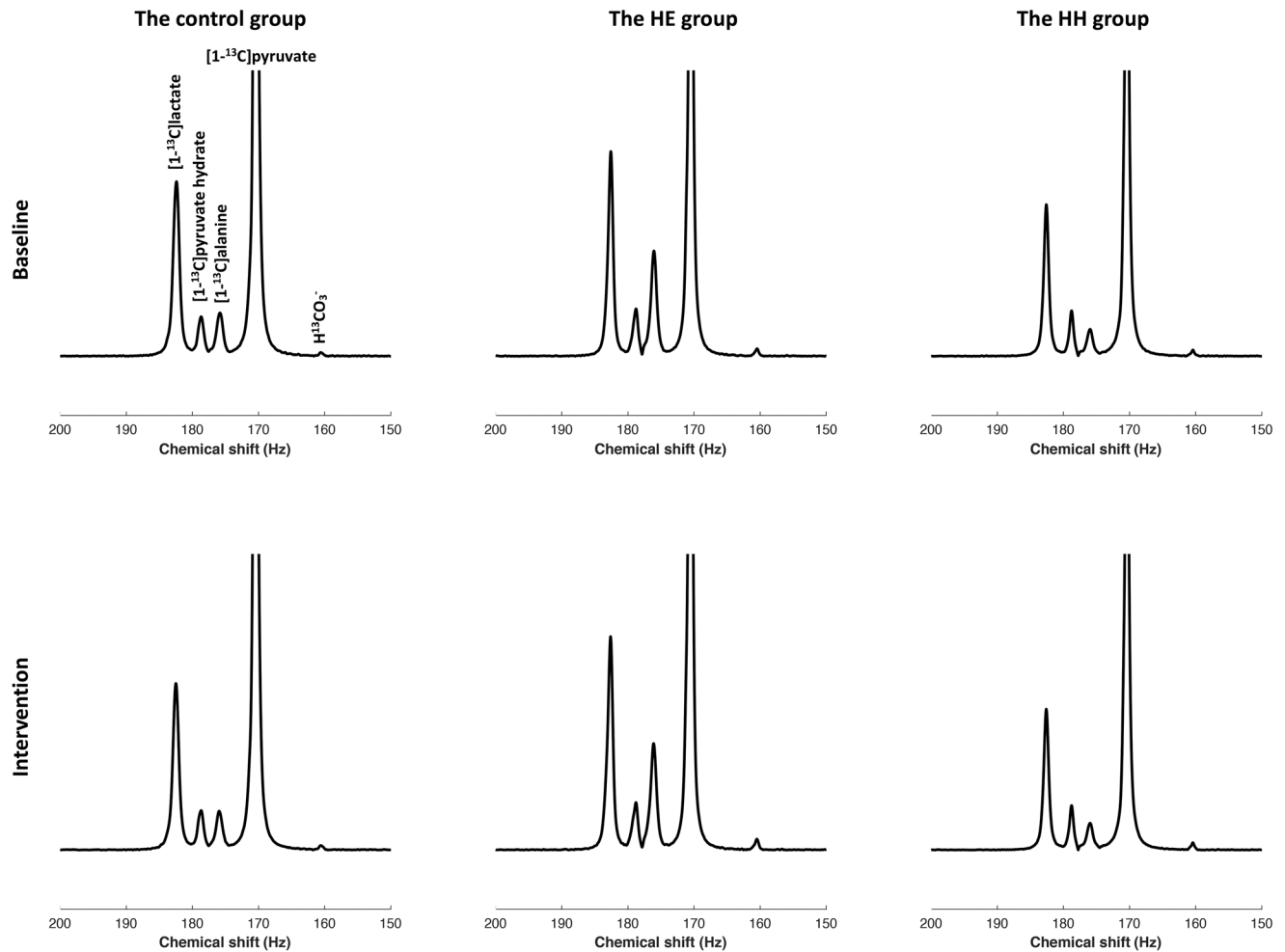


FIGURE 3 Summed spectra for the control group ($n = 4$), the hyperinsulinaemic euglycaemic group (HE group, $n = 5$) and the hyperinsulinaemic hypoglycaemic group (HH group, $n = 5$) at baseline (top spectra) and following intervention (bottom spectra), showing $[1-^{13}\text{C}]$ lactate (183 ppm), $[1-^{13}\text{C}]$ alanine (178 ppm), $[1-^{13}\text{C}]$ pyruvate (170 ppm) and ^{13}C -bicarbonate (160 ppm). The figure presents spectra where the pyruvate maximum signal peak is used to normalize the data

between the HE group and the HH group (interaction group \times time, $P = 0.06$).

3.4 | Glucose infusion rate

The GIR per kilogram (Figure 2c) increased significantly after $t = 60$ min (time, $P < 0.001$) and was statistically significantly higher in the HE group compared with the HH group (time \times group, $P = 0.03$, $P = 0.002$). The GIR at $t = 180$ min was 4.7 ± 1.2 mg/kg/min in the HE group and 3.0 ± 1.0 mg/kg/min in the HH group.

3.5 | Lactate concentrations

The HH group had consistently higher lactate concentrations (Figure 2d) throughout the study day compared with the other groups (HH group vs. control group: main effect, $P = 0.03$; interaction time \times group, $P = 0.40$; and HH group vs. HE group: main effect,

$P = 0.005$; interaction time \times group, $P = 0.82$). Lactate concentrations did not increase in the control group or the HE group during the study day (time, $P > 0.05$; interaction time \times group, $P = 0.24$).

3.6 | Hyperpolarized magnetic resonance data

The summed spectra are presented in Figure 3. Initially, we calculated the downstream metabolite to $[1-^{13}\text{C}]$ pyruvate ratios (areas under the curves). Regarding the $[1-^{13}\text{C}]$ lactate to $[1-^{13}\text{C}]$ pyruvate ratios (Figure 4a), the HH group had overall 25–50% higher ratios compared with the control group (main effect, $P = 0.003$), and the HH group did not increase more over time compared with the control group (interaction time \times group, $P = 0.19$), nor did the HE group compared with the control group (interaction time \times group, $P = 0.52$). Regarding $[1-^{13}\text{C}]$ alanine to $[1-^{13}\text{C}]$ pyruvate ratios, we found the HE and HH groups overall had higher ratios compared with the control group (HE group vs. control group, main effect $P = 0.04$; and HH group vs. control group, main effect, $P = 0.03$), but no statistically significant

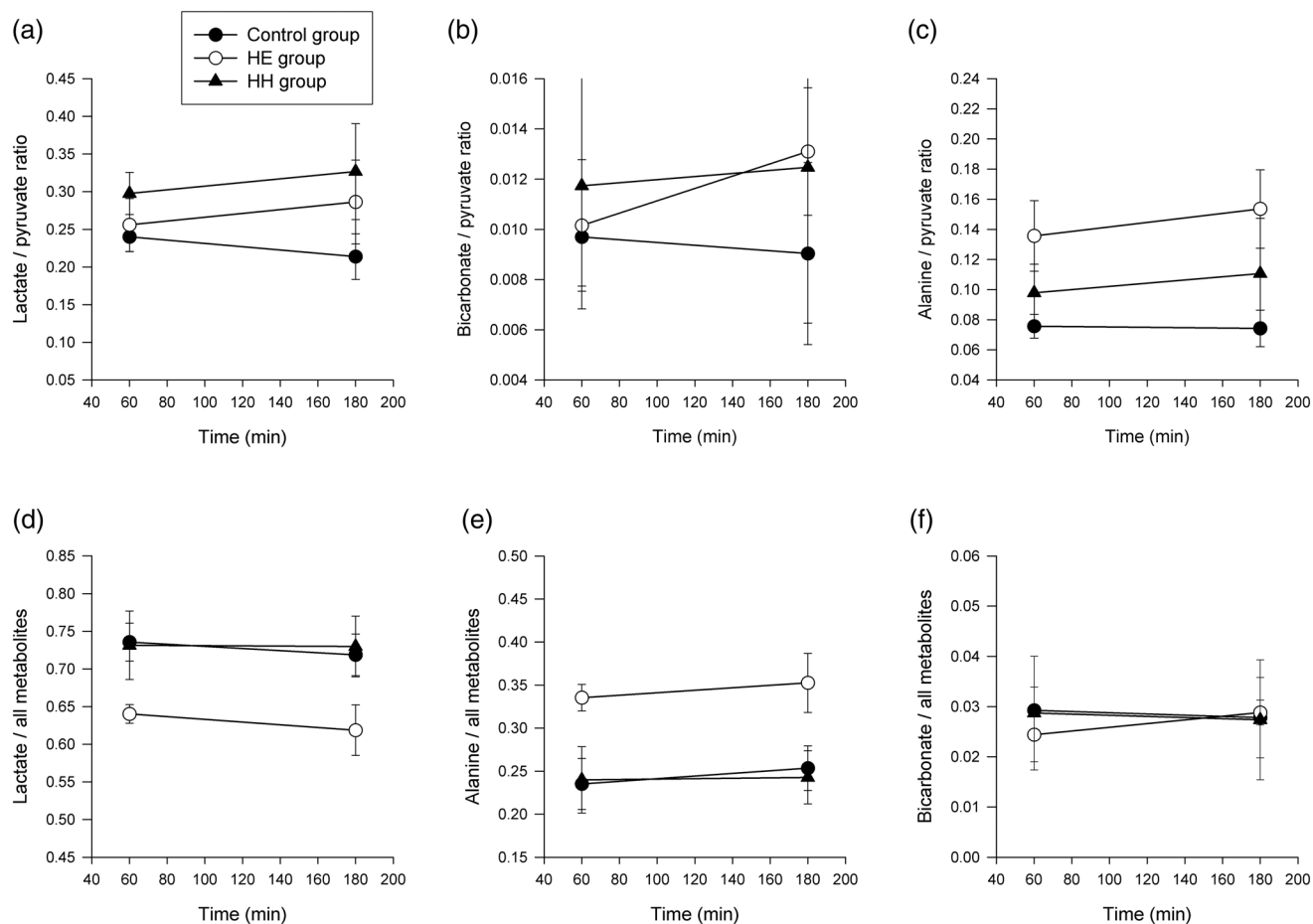


FIGURE 4 Metabolite to $[1-^{13}\text{C}]$ pyruvate ratios and metabolite ratios without $[1-^{13}\text{C}]$ pyruvate of the control group ($n = 4$), the hyperinsulinemic euglycemic group ($n = 5$) and the hyperinsulinemic hypoglycemic group ($n = 5$). $[1-^{13}\text{C}]$ Lactate to $[1-^{13}\text{C}]$ pyruvate ratio (A), ^{13}C -bicarbonate to $[1-^{13}\text{C}]$ pyruvate ratio (B) and $[1-^{13}\text{C}]$ alanine to $[1-^{13}\text{C}]$ pyruvate ratio (C), $[1-^{13}\text{C}]$ Lactate to the sum of $[1-^{13}\text{C}]$ lactate, $[1-^{13}\text{C}]$ alanine and ^{13}C -bicarbonate (D), $[1-^{13}\text{C}]$ alanine to the sum of $[1-^{13}\text{C}]$ lactate, $[1-^{13}\text{C}]$ alanine and ^{13}C -bicarbonate (E), and ^{13}C -bicarbonate to the sum of $[1-^{13}\text{C}]$ lactate, $[1-^{13}\text{C}]$ alanine and $[1-^{13}\text{C}]$ bicarbonate (F). Baseline MR hyperpolarized scan at $t = 60$ min and second scan after commenced intervention at $t = 180$ min

development over time occurred when comparing the groups (HE group vs. control group: interaction time \times group, $P = 0.23$; and HH vs. control group: interaction time \times group, $P = 0.63$). Regarding the ^{13}C -bicarbonate to $[1-^{13}\text{C}]$ pyruvate ratio, we found no significant changes over time in the HE group compared with the control group (interaction time \times group, $P = 0.12$). No statistically significant differences were present when comparing the HH group with the control group with regard to development over time (interaction time \times group, $P = 0.74$).

In order to evaluate whether the $[1-^{13}\text{C}]$ pyruvate uptake and/or metabolic conversion caused the above-mentioned differences, we calculated the downstream metabolic fractions by taking each downstream metabolite as the sum of the downstream metabolites $[1-^{13}\text{C}]$ lactate, ^{13}C -bicarbonate and $[1-^{13}\text{C}]$ alanine (Figures 4d-f). Regarding the $[1-^{13}\text{C}]$ lactate to overall metabolites, the HE group had overall lower ratios compared with the control group (main effect, $P = 0.02$), but no statistically significant differences were seen over time (interaction time \times group, $P = 0.91$). No statistically significant

differences occurred over time in the HH group compared with the control group (interaction time \times group, $P = 0.67$). Regarding the $[1-^{13}\text{C}]$ alanine to overall metabolites, we found the HE group overall had higher ratios compared with the control group (main effect, $P = 0.02$), and no statistically significant differences were found over time when comparing the groups (interaction time \times group, $P = 0.97$). Likewise, we found no statistically significant differences over time in the HH group compared with the control group (interaction time \times group, $P = 0.64$). With regard to ^{13}C -bicarbonate to overall metabolites, we observed no statistically significant differences over time when comparing the HE and HH group with the control group (HE group vs. control group: interaction time \times group, $P = 0.36$; and HH group vs. control group: interaction time \times group, $P = 0.99$).

One extra pig was included to produce hyperpolarized images of the area in the sensitivity range of the coil during a hyperinsulinaemic euglycaemic clamp, as previously described. The images were of good quality, and $[1-^{13}\text{C}]$ lactate and $[1-^{13}\text{C}]$ alanine dynamic changes was present, whereas ^{13}C -bicarbonate was below the detection level of the

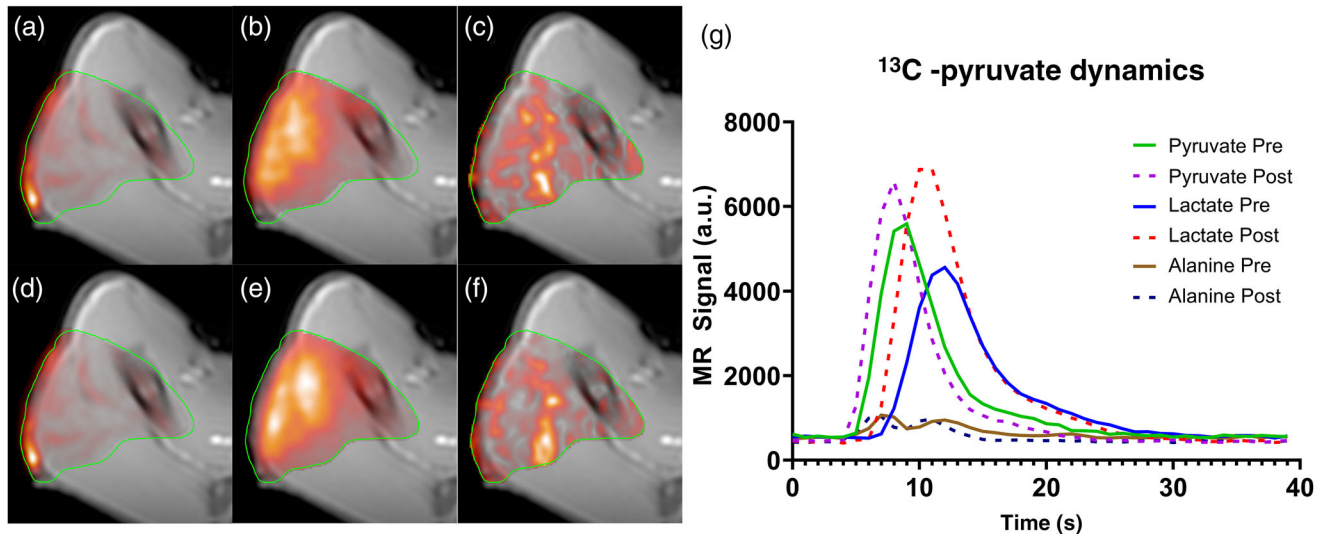


FIGURE 5 Hyperpolarized ^{13}C imaging of the lower hindlimb. The images show a signal governed by the coil sensitivity and a low penetration depth. (a–f) $[1-^{13}\text{C}]$ images overlaid on the reference ^1H anatomical image, cropped by a region of interest corresponding to signals in the graph on the right. (a) Hyperpolarized $[1-^{13}\text{C}]$ pyruvate sum image at baseline. (b) Hyperpolarized $[1-^{13}\text{C}]$ lactate sum image at baseline. (c) Hyperpolarized $[1-^{13}\text{C}]$ alanine sum image at baseline. (d) Hyperpolarized $[1-^{13}\text{C}]$ pyruvate sum image at clamp end. (e) Hyperpolarized $[1-^{13}\text{C}]$ lactate sum image at clamp end. (f) Hyperpolarized $[1-^{13}\text{C}]$ alanine sum image at clamp end. (g) Dynamic signal evolution of the hyperpolarized $[1-^{13}\text{C}]$ pyruvate, $[1-^{13}\text{C}]$ lactate and $[1-^{13}\text{C}]$ alanine over time. Abbreviations: MR, magnetic resonance; Post, after the hyperinsulinaemic euglycaemic clamp; Pre, before the hyperinsulinaemic euglycaemic clamp. $n = 1$

imaging method and not presented. The dynamics and overlaid images from this experiment are presented in Figure 5.

3.7 | Flow parameters in the scanned muscle

Using an injection of gadolinium, we measured haemodynamic parameters. Plasma flow into the skeletal muscle in the control, HE and HH groups was 73 ± 42 , 166 ± 62 and 152 ± 67 ml/100 ml/min, respectively (one-way ANOVA, $P = 0.05$). The volume distribution in the muscle in the control, HE and HH groups was 19 ± 11 , 43 ± 23 and 42 ± 18 ml/100 ml, respectively (one-way ANOVA, $P = 0.09$). The mean transit time in the muscle in the control, HE and HH groups was 18 ± 7 , 17 ± 6 and 17 ± 1 s, respectively (one-way ANOVA, $P = 0.92$).

3.8 | Insulin signalling in skeletal muscle

Western blotting was used to measure the intramuscular content of glycogen synthase (GS), As160 and AKT and their respective phosphorylated (p) forms (Figure 6). Glycogen synthase phosphorylation at s641 and total GS decreased in all groups over time (time, $P < 0.05$), with no statistically significant differences between groups (HE group vs. control group: interaction time \times group, $P = 0.43$; and HH group vs. control group: interaction time \times group, $P = 0.54$). As160 phosphorylation at thr642 and total As160 increased significantly in the HE and HH groups compared with the control group (HE group vs. control group: interaction time \times group, $P = 0.05$; and HH group vs. control group: interaction time \times group, $P < 0.001$).

The phosphorylation of AKT at serine 473 and panAKT was similar between the groups ($P > 0.05$) at baseline ($t = 0$ min) and did not increase significantly in the HE group compared with the control group (interaction time \times group, $P = 0.19$) or in the HH group compared with the control group (interaction time \times group, $P = 0.26$).

4 | DISCUSSION

During a hyperinsulinaemic euglycaemic clamp, $\sim 90\%$ of glucose uptake occurs in the skeletal muscle (Defronzo et al., 1979; Thiebaud et al., 1982). Our data showed that GIR values were substantially increased in the hyperinsulinaemic groups, and western blotting data suggested that insulin targets were stimulated. Nevertheless, we found no statistically significant differences in ratios of $[1-^{13}\text{C}]$ lactate to $[1-^{13}\text{C}]$ pyruvate, $[1-^{13}\text{C}]$ alanine to $[1-^{13}\text{C}]$ pyruvate and ^{13}C -bicarbonate to $[1-^{13}\text{C}]$ pyruvate, which are assumed to be quantitative measures of anaerobic and aerobic metabolism, when comparing our hyperinsulinaemic groups with the control group. We cannot rule out a smaller change than the sensitivity of the hMR technique allows us to capture; however, these findings suggest that hyperpolarized $[1-^{13}\text{C}]$ pyruvate is not optimally suited to detect effects of insulin in resting skeletal muscle of anaesthetized pigs.

The ^{13}C -bicarbonate production originates exclusively from pyruvate dehydrogenase flux, converting the $[1-^{13}\text{C}]$ pyruvate to ^{13}C -bicarbonate, and pyruvate carboxylase flux makes a negligible contribution to this pool. Furthermore, the non-labelled bicarbonate pool has contributions from the summed oxidation and, as indicated by the study by Jin et al. (2016), a detectable ^{13}C -bicarbonate signal in the

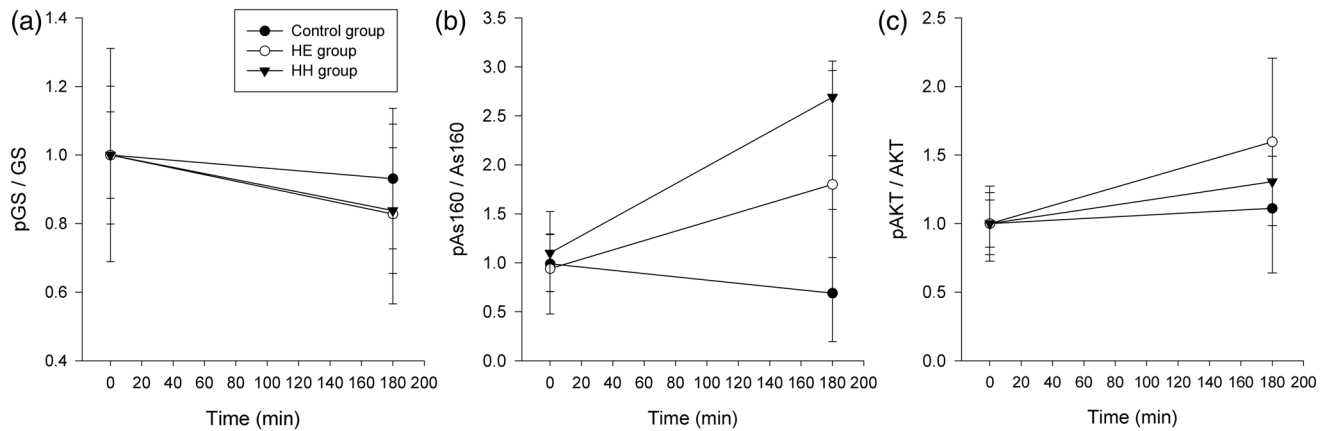


FIGURE 6 Insulin signalling in muscle tissue of the control group ($n = 5$), the hyperinsulinaemic euglycaemic group (HE group, $n = 5$) and the hyperinsulinaemic hypoglycaemic group (HH group, $n = 5$). Results are expressed as the ratio between phosphorylated protein and total protein measurements. (a) Mean ratios of phosphorylation of glycogen synthase (GS) at s641 and total GS. (b) Median ratios of phosphorylation of As160 at thr642 and total As160. (c) Mean ratios of phosphorylation of AKT at serine 473 and panAKT. Results are expressed as the ratio between phosphorylated protein and total protein measurements

rat liver seems to be present only in fed animals, not in fasted animals, leading us to speculate whether the same applies to skeletal muscle.

To the best of our knowledge, only one other study has investigated the effects of insulin in resting skeletal muscle with hyperpolarized [$1\text{-}^{13}\text{C}$]pyruvate. Leftin et al. (2013) found a nearly 100% increase in the [$1\text{-}^{13}\text{C}$]lactate to [$1\text{-}^{13}\text{C}$]pyruvate ratio after insulin stimulation of the hindlimb skeletal muscle of mice. In contrast, we observed a 10% increase in the ratio of [$1\text{-}^{13}\text{C}$]lactate to [$1\text{-}^{13}\text{C}$]pyruvate in our hyperinsulinaemic group compared with the control group. These discrepancies could be explained by differences in blood insulin concentration (hence, glucose uptake) between studies, by species differences and by modulation of metabolism induced by the anaesthetic drugs, as addressed later. We also found a 20% increase in the ^{13}C -bicarbonate to [$1\text{-}^{13}\text{C}$]pyruvate ratio (a quantitative measure of aerobic metabolism) in the HE group compared with the control group. Leftin et al. (2013) were not able to measure bicarbonate ratios owing to a low signal-to-noise ratio.

Our failure to capture any substantial metabolic effects of insulin in skeletal muscle using the hMR technique might be inherent to the methodology and model used. If both influx/appearance rates and efflux/disappearance rates of a specific metabolite in a specific biological compartment are altered (increased) to a similar extent, this would result in unaltered tracer-to-trace ratios and inability of the model to detect alterations despite profound changes in flux values.

Interestingly, we found plasma lactate concentrations to be higher overall in the HH group compared with both other groups, without dynamic changes after induced hypoglycaemia. In humans, as a counter-regulatory measure during hypoglycaemia, anaerobic glycolysis mobilizes lactate from skeletal muscle, designated to be used as a gluconeogenic substrate in the liver (Bengtson et al., 2020; Gjedsted et al., 2011). Whether the same counter-regulatory measure occurs in pigs during hypoglycaemia is unclear, as recently questioned by Gradel et al. (2020). Coherent with the overall higher blood lactate concentrations, we observed overall higher [$1\text{-}^{13}\text{C}$]lactate to [$1\text{-}^{13}\text{C}$]pyruvate ratios in skeletal muscle measured with hMR in the HH group compared with the control group and the HE group, implying a tight connectivity between blood lactate and skeletal muscle lactate.

In the present study, we assessed whether combining hMR and the hyperinsulinaemic clamp technique in a larger animal model was feasible. Performing a hyperinsulinaemic clamp in an MR scanner is a logistical challenge and requires several MR-compatible infusion pumps. We succeeded in clamping the pigs inside the MR scanner using assembled connecting tubes, enabling us to avoid moving the pigs.

Strengths of our study are that in skeletal muscle, [$1\text{-}^{13}\text{C}$]pyruvate is taken up by way of the monocarboxylate transporter (Keshari et al., 2013). In contrast to the glucose transporter GLUT4, the monocarboxylate transporters are believed not to be affected by any short-term regulation, such as insulin or other hormones (Halestrap & Price, 1999; Thiebaud et al., 1982). Furthermore, hyperpolarized [$1\text{-}^{13}\text{C}$]pyruvate images showed detectable signal on [$1\text{-}^{13}\text{C}$]lactate and [$1\text{-}^{13}\text{C}$]alanine produced in the nearby muscle. The metabolite ^{13}C -bicarbonate was below the detection limit, which is in agreement with Leftin et al. (2013). It shows promise for human studies, including studies on actively working muscle, where the metabolism is higher.

Limitations should be noted. The present design was based upon previous hMR studies in pigs, where $n = 4$ in each group have shown profound metabolic changes in striated cardiac muscle with a similar intervention (Hansen et al., 2017). Furthermore, from human trials we have learned that $n = 6$ is enough to show substantial effects on glucose metabolism in skeletal muscle using the hyperinsulinaemic clamp technique (Mose et al., 2020). Nevertheless, it is not optimal that the groups sizes are based on empirical knowledge rather than on power calculations. Future studies might benefit from the data accrued in the present study, with sample sizes planned accordingly. Nonetheless, the metabolic changes we observe in our hMR data are subtle compared with the only other published study examining the effects of insulin in skeletal muscle (Leftin et al., 2013), and we therefore suspect that the general anaesthesia has induced skeletal muscle insulin resistance

and obstructed our ability to record significant metabolic changes. In support of this, in humans, general anaesthetic procedures have been shown to induce an extensive inhibition of substrate oxidation in muscle mitochondria, and anaesthetic drugs are known to increase blood glucose concentrations (Manell et al., 2017; Miró et al., 1999). In future studies, it would be of interest to measure concentrations of pyruvate, lactate and alanine in both blood and muscle, providing further insight into the metabolism, in addition to investigating the enrichment of ^{13}C in the glycogen pool, as previously done by Heinicke et al. (2014). We experienced unexpected differences in baseline data between the groups, suspected to be attributable to data outliers, which is a well-known phenomenon in studies with parallel groups and low n . A randomized cross-over design without the interference of anaesthesia in order to reduce inter-individual differences is preferable in a future human trial.

With the application of a gadolinium injection, we computed blood flow to the muscle. This revealed higher flows in our hyperinsulinaemic groups compared with the control group, implying that clamp conditions increase blood flow. This is a finding discussed by Høiegggen et al. (1999) and certainly an observation of note for future hMR studies.

4.1 | Conclusion

Our study is the first of its kind, combining hMR and the hyperinsulinaemic clamp model and including western blot of muscle tissue biopsies. We report substantial increments in GIR, representing skeletal muscle glucose uptake, in addition to phosphorylated insulin targets, but found no statistically significant differences in the ratios of $[1-^{13}\text{C}]\text{lactate}$ to $[1-^{13}\text{C}]\text{pyruvate}$, $[1-^{13}\text{C}]\text{alanine}$ to $[1-^{13}\text{C}]\text{pyruvate}$ and ^{13}C -bicarbonate to $[1-^{13}\text{C}]\text{pyruvate}$, which are assumed to be quantitative measures of anaerobic and aerobic metabolism, when comparing our hyperinsulinaemic groups with the control group. These findings imply that the hyperpolarization technique might not be optimal for detecting effects of insulin in anaesthetized skeletal muscle, which is noteworthy for future studies. Although our primary outcome showed no statistically significant differences, the study adds several aspects to the field of metabolic experimental research, promotes minimally invasive methods and highlights several important issues to consider in the imminent human trials involving hMR.

ACKNOWLEDGEMENTS

We would like to thank K. Nyborg Rasmussen, E. Søgaard Hornemann, Z. Pertovi Nasr and L. Kvist of the Medical Research Laboratories and H. Zibrandtsen of the Research Laboratories for Biochemical Pathology at Aarhus University Hospital, Denmark for their excellent technical assistance and guidance. The present research projects were financially supported by Aarhus University, Denmark and by Innovation Fund Denmark, project LIFE-DNP: Hyperpolarized Magnetic Resonance For In Vivo Of Lipid, Sugar And Amino Acid Metabolism In Lifestyle Related Diseases, grant number 1308-00028B.

COMPETING INTERESTS

None declared.

AUTHOR CONTRIBUTIONS

M.B.B., J.S., N.F.R., N.M., E.S.S.H., R.S.T., H.S.-J., R.S.T. and C.L. designed the study. M.B.B., E.S.S.H., R.S.T., C.Ø.M. and M.D.L. conducted the trial. M.B.B. conducted the statistical analyses. M.B.B., N.M., E.S.S.H. and C.L. wrote the manuscript. J.S., N.F.R., R.S.T., H.S.-J., N.J., C.Ø.M. and M.D.L. reviewed and edited the manuscript. C.L. is the guarantor of this work and, as such, had full access to all the data in the study and takes responsibility for the integrity of the data and the accuracy of the data analysis. All authors approved the final version of the manuscript and agree to be accountable for all aspects of the work in ensuring that questions related to the accuracy or integrity of any part of the work are appropriately investigated and resolved. All persons designated as authors qualify for authorship, and all those who qualify for authorship are listed.

DATA AVAILABILITY STATEMENT

Data are available at: Bengtson, M. B. (2021): Hyperpolarized $[1-^{13}\text{C}]\text{pyruvate}$ combined with the hyperinsulinaemic euglycaemic and hypoglycaemic clamp technique in skeletal muscle in a large animal model. <https://doi.org/10.6084/m9.figshare.16688782.v1>

ORCID

Mads Bisgaard Bengtson  <https://orcid.org/0000-0001-8985-8385>

Rasmus Stilling Tougaard  <https://orcid.org/0000-0003-2199-0405>

Mads Dam Lyhne  <https://orcid.org/0000-0001-5279-260X>

Christoffer Laustsen  <https://orcid.org/0000-0002-0317-2911>

REFERENCES

- Ardenkjær-Larsen, J. H., Fridlund, B., Gram, A., Hansson, G., Hansson, L., Lerche, M. H., Servin, R., Thaning, M., & Golman, K. (2003). Increase in signal-to-noise ratio of > 10,000 times in liquid-state NMR. *Proceedings of the National Academy of Sciences of the United States of America*, 100, 10158–10163. <https://doi.org/10.1073/pnas.1733835100>
- Bengtson, M. B., Støy, J., Rittig, N. F., Voss, T. S., Magnusson, N. E., Svart, M. V., Jessen, N., & Møller, N. (2020). A human randomized controlled trial comparing metabolic responses to single and repeated hypoglycemia in type 1 diabetes. *Journal of Clinical Endocrinology and Metabolism*, 105, dgaa645. <https://doi.org/10.1210/clinem/dgaa645>
- Bergstrom, J. (1975). Percutaneous needle biopsy of skeletal muscle in physiological and clinical research. *Scandinavian Journal of Clinical and Laboratory Investigation*, 35, 609–616. <https://doi.org/10.1080/00365517509095787>
- DeFronzo, R. A., & Tripathy, D. (2009). Skeletal muscle insulin resistance is the primary defect in type 2 diabetes. *Diabetes Care*, 32, 157–162. <https://doi.org/10.2337/dc09-s302>
- DeFronzo, R. A., Tobin, J. D., & Andres, R. (1979). Glucose clamp technique: A method for quantifying insulin secretion and resistance. *The American Journal of Physiology*, 237, E214–E223. <https://doi.org/10.1152/ajpendo.1979.237.3.e214>
- Gilda, J. E., & Gomes, A. V. (2013). Stain-Free total protein staining is a superior loading control to β -actin for Western blots. *Analytical Biochemistry*, 440, 186–188. <https://doi.org/10.1016/j.ab.2013.05.027>
- Gjedsted, J., Buhl, M., Nielsen, S., Schmitz, O., Vestergaard, E. T., Tønnesen, E., & Møller, N. (2011). Effects of adrenaline on lactate, glucose, lipid and protein metabolism in the placebo controlled bilaterally perfused

- human leg. *Acta Physiologica*, 202, 641–648. <https://doi.org/10.1111/j.1748-1716.2011.02316.x>
- Gradel, A. K. J., Kildegaard, J., Ludvigsen, T. P., Porsgaard, T., Schou-Pedersen, A. M. V., Fels, J. J., Lykkesfeldt, J., & Refsgaard, H. H. F. (2020). The counterregulatory response to hypoglycaemia in the pig. *Basic & Clinical Pharmacology & Toxicology*, 127(4), 278–286. <https://doi.org/10.1111/bcpt.13422>
- Halestrap, A. P., & Price, N. T. (1999). The proton-linked monocarboxylate transporter (MCT) family: Structure, function and regulation. *The Biochemical Journal*, 343(Pt 2), 281–299. <http://www.ncbi.nlm.nih.gov/pmc/articles/pmc1220552/>
- Hansen, E. S. S., Tougaard, R. S., Nørlinger, T. S., Mikkelsen, E., Nielsen, P. M., Bertelsen, L. B., Bøtker, H. E., Jørgensen, H. S., & Laustsen, C. (2017). Imaging porcine cardiac substrate selection modulations by glucose, insulin and potassium intervention: A hyperpolarized [^{1-13}C]pyruvate study. *NMR in Biomedicine*, 30(6), 10.1002/nbm.3702. <https://doi.org/10.1002/nbm.3702>
- Heinicke, K., Dimitrov, I. E., Romain, N., Cheshkov, S., Ren, J., Malloy, C. R., & Haller, R. G. (2014). Reproducibility and absolute quantification of muscle glycogen in patients with glycogen storage disease by ^{13}C NMR spectroscopy at 7 Tesla. *PLoS One*, 9(10), e108706. <https://doi.org/10.1371/journal.pone.0108706>
- Højeggen, A., Fossum, E., Moan, A., Rostrup, M., Eide, I. K., & Kjeldsen, S. E. (1999). Increased forearm blood flow during glucose clamp is related neither to insulin sensitivity nor to hyperinsulinemia in borderline hypertensive young men. *Blood Pressure*, 4, 227–230. <https://doi.org/10.1080/080370599439616>
- Jensen, J., Rustad, P. I., Kolnes, A. J., & Lai, Y. C. (2011). The role of skeletal muscle glycogen breakdown for regulation of insulin sensitivity by exercise. *Frontiers in Physiology*, 2, 112. <https://doi.org/10.3389/fphys.2011.00112>
- Jin, E. S., Moreno, K. X., Wang, J. X., Fidelino, L., Merritt, M. E., Sherry, A. D., & Malloy, C. R. (2016). Metabolism of hyperpolarized [^{1-13}C]pyruvate through alternate pathways in rat liver. *NMR in Biomedicine*, 29(4), 466–474. <https://doi.org/10.1002/nbm.3479>. Epub 2016 Feb 2. PMID: 26836042; PMCID: PMC4805436.
- Juel, C., & Halestrap, A. (1999). Lactate transport in skeletal muscle – role and regulation of the monocarboxylate transporter. *The Journal of Physiology*, 517(3), 633–642. <https://doi.org/10.1111/j.1469-7793.1999.0633s.x>
- Keshari, K. R., Sriram, R., van Criekinge, M., Wilson, D. M., Wang, Z. J., Vigneron, D. B., Peehl, D. M., & Kurhanewicz, J. (2013). Metabolic reprogramming and validation of hyperpolarized ^{13}C lactate as a prostate cancer biomarker using a human prostate tissue slice culture bioreactor. *The Prostate*, 73, 1171–1181. <https://doi.org/10.1002/pros.22665>
- Khegai, O., Schilte, R. F., Janich, M. A., Menzel, M. I., Farrell, E., Otto, A. M., Ardenkjaer-Larsen, J. H., Glaser, S. J., Haase, A., Schwaiger, M., & Wiesinger, F. (2014). Apparent rate constant mapping using hyperpolarized [^{1-13}C]pyruvate. *NMR in Biomedicine*, 27, 1256–1265. <https://doi.org/10.1002/nbm.3174>
- Lauritzen, M. H., Laustsen, C., Butt, S. A., Magnusson, P., Søgaard, L. V., Ardenkjaer-Larsen, J. H., & Åkeson, P. (2013). Enhancing the [^{13}C]bicarbonate signal in cardiac hyperpolarized [^{1-13}C]pyruvate MRS studies by infusion of glucose, insulin and potassium. *NMR in Biomedicine*, 26, 1496–1500. <https://doi.org/10.1002/nbm.2982>
- Leftin, A., Degani, H., & Frydman, L. (2013). In vivo magnetic resonance of hyperpolarized [$^{13}\text{C}_1$]pyruvate: Metabolic dynamics in stimulated muscle. *American Journal of Physiology. Endocrinology and Metabolism*, 305, E1165–E1171. <https://doi.org/10.1152/ajpendo.00296.2013>
- Manell, E., Jensen-Waern, M., & Hedenqvist, P. (2017). Anaesthesia and changes in parameters that reflect glucose metabolism in pigs – a pilot study. *Laboratory Animals*, 51(5), 509–517. <https://doi.org/10.1177/0023677216682773>
- Miró, O., Barrientos, A., Alonso, J. R., Casademont, J., Jarreta, D., Urbano-Márquez, A., & Cardellach, F. (1999). Effects of general anaesthetic procedures on mitochondrial function of human skeletal muscle. *European Journal of Clinical Pharmacology*, 55(1), 35–41. <https://doi.org/10.1007/s002280050589>
- Mose, M., Rittig, N., Mikkelsen, U. R., Jessen, N., Bengtsen, M. B., Christensen, B., Jørgensen, J., & Møller, N. (2020). A model mimicking catabolic inflammatory disease; a controlled randomized study in humans. *PLoS One*, 15(11), e0241274. <https://doi.org/10.1371/journal.pone.0241274>
- Park, J. M., Hackett, E. P., Harrison, C. E., Reed, G. D., Chhabra, A., & Malloy, C. R. (2020). Effects of anaerobic exercise in skeletal muscle measured by hyperpolarized [^{1-13}C]pyruvate in humans. ISMRM and SMRT, Virtual conference and exhibition, 8–14 August 2020. abstract number 3000. URL: https://www.ismrm.org/20/program_files/DP07-01.htm
- Nielsen, P. M., Mariager, C. Ø., Mølmer, M., Sparding, N., Genovese, F., Karsdal, M. A., Nørregaard, R., & Laustsen, C. (2020). Hyperpolarized [^{1-13}C] alanine production: A novel imaging biomarker of renal fibrosis. *Magnetic Resonance in Medicine*, 84(4), 2063–2073. <https://doi.org/10.1002/mrm.28326>. Epub 2020 May 25. PMID: 32452096
- Shulman, G. I., Rothman, D. L., Jue, T., Stein, P., DeFronzo, R. A., & Shulman, R. G. (1990). Quantitation of muscle glycogen synthesis in normal subjects and subjects with non-insulin-dependent diabetes by ^{13}C nuclear magnetic resonance spectroscopy. *The New England Journal of Medicine*, 322(4), 223–228. <https://doi.org/10.1056/NEJM199001253220403>
- Swanson, K. S., Mazur, M. J., Vashisht, K., Rund, L. A., Beever, J. E., Counter, C. M., & Schook, L. B. (2004). Genomics and clinical medicine: Rationale for creating and effectively evaluating animal models. *Experimental Biology and Medicine*, 229(9), 866–875. <https://doi.org/10.1177/153537020422900902>
- Thiebaud, D., Jacot, E., DeFronzo, R. A., Maeder, E., Jequier, E., & Felber, J. P. (1982). The effect of graded doses of insulin on total glucose uptake, glucose oxidation, and glucose storage in man. *Diabetes*, 31(11), 957–963. <https://doi.org/10.2337/diacare.31.11.957>
- Torchi, A., Serres, S., Cooper, A., Mallinson, J., McGing, J., Lobo, D. N., Cooper, A., Awais, R., Årstad, E., Glaser, M., Twyman, F., Gowland, P., Auer, D., Greenhaff, P. L., Faas, H., & Morris, P. (2019). Monitoring muscle metabolism non-invasively with dynamic nuclear polarisation magnetic resonance. WMIC 2019 in Montreal, 4–8 September 2019. Abstract number 538, URL: <https://www.xcdsystem.com/wmic/program/wtcFzFz/index.cfm?pgid=1223>
- Zöllner, F. G., Daab, M., Sourbron, S. P., Schad, L. R., Schoenberg, S. O., & Weisser, G. (2016). An open source software for analysis of dynamic contrast enhanced magnetic resonance images: UMMPerfusion revisited. *BMC Medical Imaging*, 16, 7. <https://doi.org/10.1186/s12880-016-0109-0>

SUPPORTING INFORMATION

Additional supporting information may be found in the online version of the article at the publisher's website.

How to cite this article: Bengtsen, M. B., Hansen, E. S. S., Tougaard, R. S., Lyhne, M. D., Rittig, N. F., Støy, J., Jessen, N., Mariager, C. Ø., Stødkilde-Jørgensen, H., Møller, N., & Laustsen, C. (2021). Hyperpolarized [^{1-13}C]pyruvate combined with the hyperinsulinaemic euglycaemic and hypoglycaemic clamp technique in skeletal muscle in a large animal model. *Experimental Physiology*, 106, 2412–2422. <https://doi.org/10.1113/EP089782>